Dalton Transactions

ROYAL SOCIETY OF CHEMISTRY

COMMUNICATION

View Article Online
View Journal | View Issue

Cite this: *Dalton Trans.*, 2026, **55**, 4402

Received 7th January 2026,
Accepted 24th February 2026

DOI: 10.1039/d6dt00040a

rsc.li/dalton

Realization of the transition from an indirect band gap to a direct band gap through halogen regulation in the Cs–Ag–X system

Bingliang Cheng,†[a,b] Wenjuan Ma,†[c] Cong Hu,[b] Yuhan Lv,[b] Zongxiao Li,[b] Jianchao Zhao,[b] Tao Bo [a,b] and Wenwen Lin *[a,b]

Scintillation crystals need to have a direct band gap. Here, two new optical crystals, CsAgICl and Cs_2AgBr_2I, were obtained through halogen regulation, achieving the transition from an indirect band gap ($CsAgCl_2$) to a direct band gap. This work enriches the structural chemistry of the Cs–Ag–X system and is conducive to the exploration of new scintillation crystals.

Nuclear radiation detection crystals are the core materials of detection devices and have significant applications in medical diagnosis, security screening, high-energy physics, and homeland safety.[1–4] The metal halide perovskite $CsPbBr_3$ has attracted much attention due to its excellent photon-to-electron conversion efficiency, high defect tolerance factor, and high carrier mobility-lifetime product.[5–7] However, the $CsPbBr_3$ crystal has encountered some inherent problems, such as the toxicity of Pb and ionic migration caused by its three-dimensional (3D) structure, which restricts its environmental friendliness and long-term performance.[8–13]

In recent years, considering the limitations imposed by the aforementioned various challenges, other lead-free alternative materials, such as $Cs_3Cu_2I_5$, $Cs_2AgBiBr_6$, $Cs_3Bi_2I_9$, *etc.*, have also been studied and explored.[14–20] Their superior stability and environmentally friendly characteristics have attracted widespread attention and achieved rapid development, demonstrating excellent performance in all-inorganic nuclear radiation detection. For these lead-free systems, research on the silver halide Cs–Ag–X system is relatively scarce.[21,22] Among them, $CsAg_2I_3$ has been reported to have an excellent UV photodetector response speed, due to the $[Ag_2X_6]$ octahedral units in its structure.[23]

In this work, based on the halogen regulation strategy, two new Ag-based halides with $[AgX_4]$ units were obtained, namely CsAgICl and Cs_2AgBr_2I. Compared with the known $CsAgCl_2$, the main framework of CsAgICl is a layered structure composed of $[AgCl_2I_2]$ units, while the anionic framework of Cs_2AgBr_2I is a 1D $[AgBr_2I]_\infty$ chain structure composed of $[AgBr_2I_2]$ units. Meanwhile, the introduction of Br and I changed the coordination environment of the Ag atom from 5-coordination in $CsAgCl_2$ to 4-coordination in CsAgICl and Cs_2AgBr_2I. Unfortunately, the $[AgCl_2I_2]$ unit and the $[AgBr_2I_2]$ unit failed to form the $[Ag_2X_6]$ octahedral unit with enhanced luminescence properties through edge-sharing connection modes. The results of first-principles calculations indicate that the change of halogen regulates the band gap and realizes the transition from an indirect band gap ($CsAgCl_2$) to a direct band gap (CsAgICl and Cs_2AgBr_2I). These results will open a new avenue for exploring nuclear radiation detection materials in the Cs–Ag–X system with direct band gaps.

Single crystals of CsAgICl and Cs_2AgBr_2I were obtained by a high-temperature solid-state method in a vacuum system, and their polycrystalline samples (Fig. S1) can be prepared by solid-state and antisolvent methods (experimental details are presented in the SI). Compared with the solid-state method, the antisolvent method for synthesizing polycrystalline samples is more time-efficient. The purity of the phase was determined by powder X-ray diffraction (XRD) (Fig. 1d and f). Meanwhile, to compare the effect of halogen regulation on the band gap, polycrystalline samples of $CsAgCl_2$ were synthesized. Compared with the previously reported synthesis of $CsAgCl_2$ nanocrystals using the anti-solvent method,[21] the crystals synthesized in this study through the supersaturation method have significantly larger sizes, resulting in micron-sized single crystals (Fig. 1a and b). Crystallographic data of CsAgICl and Cs_2AgBr_2I are presented in Table S1. Their bond lengths and bond angles are comparable to those of known metal halides (Tables S3 and S4). The rationality of the two structures was

[a]*Qianwan Institute of CNITECH, Ningbo 315336, China.*
E-mail: linwenwen@nimte.ac.cn
[b]*Zhejiang Key Laboratory of Data-Driven High-Safety Energy Materials and Applications, Ningbo Key Laboratory of Special Energy Materials and Chemistry, Ningbo Institute of Materials Technology and Engineering, Chinese Academy of Sciences, Ningbo 315201, China*
[c]*College of Physical Science and Technology, Department of Physics, Xiamen University, Xiamen 361005, China*
†These authors contributed equally to this work.

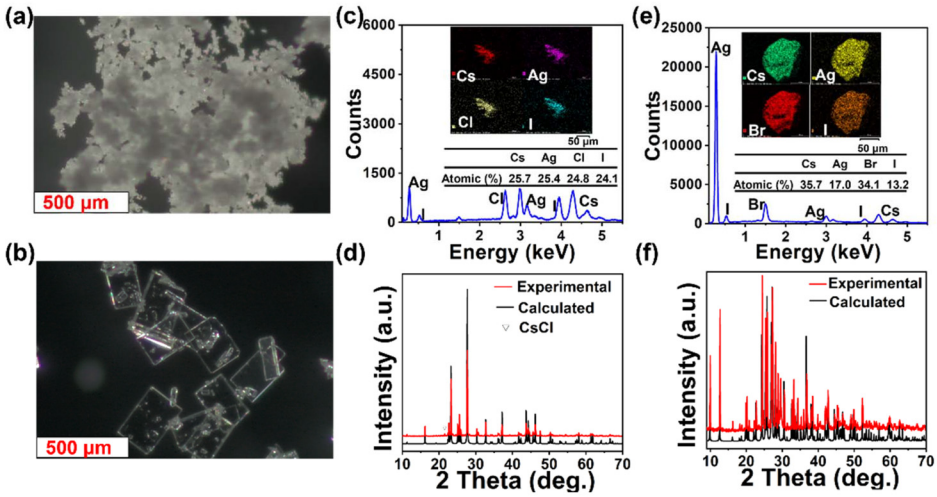

Fig. 1 Microscopic morphology of $CsAgCl_2$ obtained by (a) the antisolvent method and (b) the supersaturation method. (c) Energy dispersive spectroscopy analysis and (d) experimental powder XRD patterns of CsAgICl. (e) Energy dispersive spectroscopy analysis and (f) experimental powder XRD patterns of Cs_2AgBr_2I.

confirmed by energy dispersive spectroscopy (Fig. 1c and e) and bond valence calculation[24] (Table S2).

Two novel Ag-based halides, CsAgICl and Cs_2AgBr_2I, were obtained by introducing Br/I atoms into the $CsAgCl_2$ structure. CsAgICl crystallizes in the centrosymmetric space group *Cmcm*, which is the same as that of $CsAgCl_2$. Its cell parameters are a = 4.8341(4) Å, b = 15.6709(13) Å, c = 7.6430(5) Å, and Z = 4. In the asymmetric unit, there is one crystallographically independent Cs atom, one Ag atom, one Cl atom, and one I atom. The central atom Ag is coordinated to two Cl atoms and two I atoms to form the $[AgCl_2I_2]$ fundamental building block (FBB) (Fig. 2b) with d_{Ag-Cl} = 2.646 Å and d_{Ag-I} = 2.764 Å. The introduction of larger-sized I atoms alters the coordination of the Ag atoms in the $[AgCl_5]$ unit of $CsAgCl_2$ (Fig. 2a). The Cs atom is coordinated to four Cl atoms and four I atoms to form a $[CsCl_4I_4]$ polyhedron. The bond lengths of d_{Cs-Cl} and d_{Cs-I} in the $[CsCl_4I_4]$ polyhedron are 3.482 Å and 3.884–4.124 Å, respectively. The formed $[AgCl_2I_2]$ units polymerize to form 2D $[AgICl]_\infty$ layers through corner-sharing. These layers extend in the *bc* plane and are connected by $[CsCl_4I_4]$ polyhedra. Finally, the overall structure of CsAgICl is composed of 2D $[AgICl]_\infty$ layers and Cs atoms (Fig. 2b). The difference from the layer structure of $CsAgCl_2$ (Fig. 2a) is that the layers of CsAgICl are not flat. Specifically, when viewed along the *a*-axis, the angle of Cl–Ag–Cl in CsAgICl is 92.447°, while in $CsAgCl_2$, it is 162.050°.

Cs_2AgBr_2I crystallizes in the centrosymmetric space group *Pnma*, which is different from that of $CsAgCl_2$. Its cell parameters are a = 10.0800(16) Å, b = 4.8981(8) Å, c = 19.635(3) Å, and Z = 4. In the asymmetric unit, there are two crystallogra-

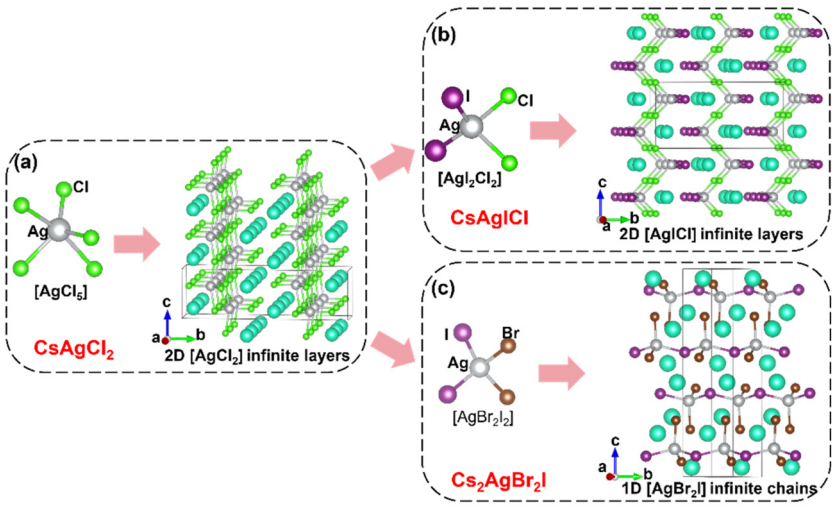

Fig. 2 Crystal structures: (a) $CsAgCl_2$, (b) CsAgICl, and (c) Cs_2AgBr_2I.

phically independent Cs atoms, one Ag atom, two Br atoms, and one I atom. The central atom Ag is coordinated to two Br atoms and two I atoms to form the $[AgBr_2I_2]$ FBB (Fig. 2c), with d_{Ag-Br} = 2.717–2.724 Å and d_{Ag-I} = 2.834 Å, which is different from the $[AgCl_5]$ FBB of $CsAgCl_2$. The Cs (1) atom is coordinated to four Br atoms and three I atoms to form a $[CsBr_4I_3]$ polyhedron, and the bond lengths of d_{Cs-Br} and d_{Cs-I} in the $[CsBr_4I_3]$ polyhedron are 3.561–3.629 Å and 3.859–3.889 Å, respectively. The Cs (2) atom is coordinated to six Br atoms and one I atom to form a $[CsBr_6I]$ polyhedron, and the bond lengths of d_{Cs-Br} and d_{Cs-I} in the $[CsBr_6I]$ polyhedron are 3.612–3.658 Å and 3.861 Å, respectively. The formed $[AgBr_2I_2]$ units polymerize to form 1D $[AgBr_2I]_\infty$ chains through I atoms, with the Br atoms being suspended. These chains extend along the *b*-axis and are connected by $[CsBr_4I_3]$ and $[CsBr_6I]$ polyhedra. Finally, the overall structure of Cs_2AgBr_2I is composed of 1D $[AgBr_2I]_\infty$ chains and Cs atoms (Fig. 2c). The introduction of Br and I atoms has transformed the layer structure of $CsAgCl_2$ into the chain structure of Cs_2AgBr_2I.

The band gap is a key parameter of optical crystals,[25–27] and the UV-vis spectra of $CsAgCl_2$ (Fig. S2), CsAgICl (Fig. 3a) and Cs_2AgBr_2I (Fig. 3d) were tested by the Tauc plot method.[28] The results show that the experimental band gap of $CsAgCl_2$ is 4.17 eV, which is consistent with previous reports,[21] and the band gaps of CsAgICl and Cs_2AgBr_2I are 2.82 eV and 3.53 eV, respectively. Furthermore, the previous reports indicate that $CsAgCl_2$ has an indirect band gap with a calculated value of 3.82 eV (Fig. S3),[21] while first-principles calculations in this work indicate that CsAgICl and Cs_2AgBr_2I have direct band gaps with values of 2.30 eV and 2.73 eV, respectively (Fig. 3b and e). The introduction of Br atoms and I atoms with weaker electronegativity can effectively reduce the band gap, which is consistent with the result that halogens regulate the band gap of optical crystals. The contribution of the orbitals to the band gap was analyzed through partial density of states (PDOS) and integrated projected density of states (IPDOS, ranging from −2.0 to 0.0 eV). For CsAgICl, near the Fermi level, the contributions of the Ag-4d, Cl-3p, and I-5p orbitals to the top of valence bands are 43%, 27%, and 26%, respectively, while the Ag-5s orbitals contribute the most to the bottom of conduction bands, which is 50% (Fig. 3c). The calculated results of Cs_2AgBr_2I are similar. The Ag-4d, Br-4p, and I-5p orbitals contribute the most to the top of valence bands, accounting for 26%, 49% and 20%, respectively, while the Ag-5s orbitals contribute 44% to the bottom of conduction bands (Fig. 3f). By comparing the PDOS of these three compounds, it can be seen that the optical band gap is mainly determined by the $[AgX_n]$ units. The introduction of different halogen atoms alters the coordination environment (from the $[AgCl_5]$ unit in $CsAgCl_2$ to the $[AgCl_2I_2]$ unit in CsAgICl and the $[AgBr_2I_2]$ unit in Cs_2AgBr_2I) and the distribution of electronic orbitals of the Ag atom, causing the wave vector positions of the conduction band bottom and the valence band top to tend to overlap, thus transforming from an indirect band gap to a direct band gap. Therefore, the introduction of Br/I atoms in this work transformed the indirect band gap into a direct band gap, which is a prerequisite for scintillation crystals.

In conclusion, two new metal halide compounds, CsAgICl and Cs_2AgBr_2I, were obtained through halogen regulation, and their polycrystalline samples were synthesized through solid-state and antisolvent methods. Meanwhile, micron-sized single crystals of $CsAgCl_2$ were grown through the supersaturation method. Furthermore, the optical band gaps and electron structures were characterized and analyzed through experiments and calculations. The results show that the introduction of different halogens can effectively regulate the band gap, converting the indirect band gap to the direct band gap, which will boost the discovery of new metal halide scintillation materials.

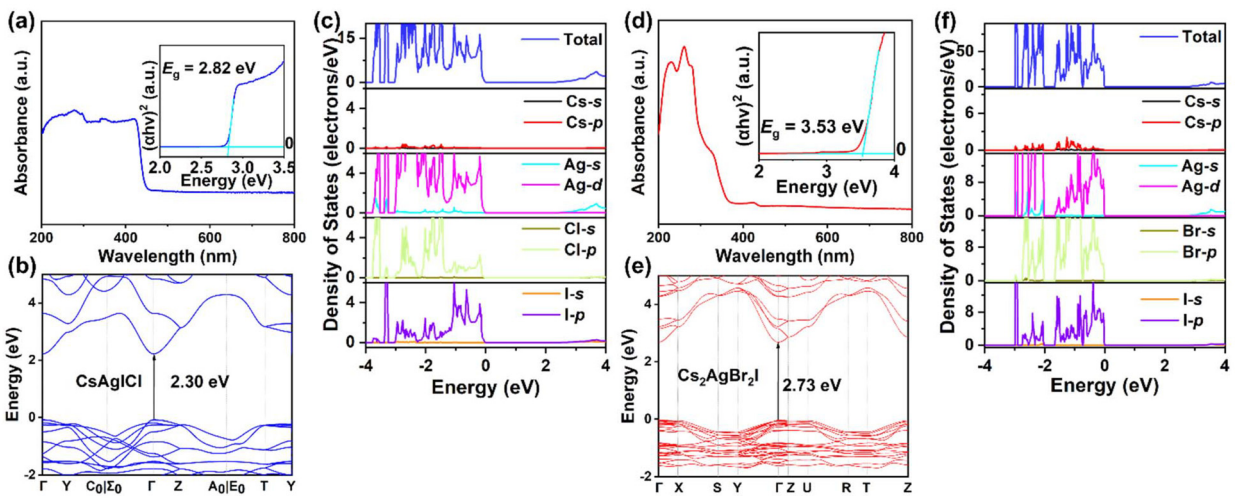

Fig. 3 (a) UV-vis optical absorption spectrum, (b) calculated band gap, and (c) calculated density of states of CsAgICl. (d) UV-vis optical absorption spectrum, (e) calculated band gap, and (f) calculated density of states of Cs_2AgBr_2I.

Conflicts of interest

The authors declare no competing financial interest.

Data availability

The data supporting this article have been included as part of the supplementary information (SI). Supplementary information: details of synthesis and characterization of compounds (PDF). See DOI: https://doi.org/10.1039/d6dt00040a.

CCDC 2519961 and 2519962 contain the supplementary crystallographic data for this paper.[29a,b]

Acknowledgements

This work was financially supported by the National Natural Science Foundation of China (52272171) and the Ningbo Yongjiang Talent Introduction Project (2021A-106-G).

References

1 Y. H. He, M. Petryk, Z. F. Liu, D. G. Chica, I. Hadar, C. Leak, W. J. Ke, I. Spanopoulos, W. W. Lin, D. Y. Chung, B. W. Wessels, Z. He and M. G. Kanatzidis, *Nat. Photonics*, 2021, **15**, 36–42.
2 Y. H. He, L. Matei, H. J. Jung, K. M. McCall, M. Chen, C. C. Stoumpos, Z. F. Liu, J. A. Peters, D. Y. Chung, B. W. Wessels, M. R. Wasielewski, V. P. Dravid, A. Burger and M. G. Kanatzidis, *Nat. Commun.*, 2018, **9**, 1609.
3 J. P. Deng, J. L. Li, Z. Yang and M. Q. Wang, *J. Mater. Chem. C*, 2019, **7**, 12415–12440.
4 Q. Xu, J. Wang, W. Y. Shao, X. Ouyang, X. Wang, X. L. Zhang, Y. Guo and X. P. Ouyang, *Nanoscale*, 2020, **12**, 9727–9732.
5 W. W. Lin, J. G. He, K. M. McCall, C. C. Stoumpos, Z. F. Liu, I. Hadar, S. Das, H. H. Wang, B. X. Wang, D. Y. Chung, B. W. Wessels and M. G. Kanatzidis, *Adv. Funct. Mater.*, 2021, **31**, 2006635.
6 Y. Wu, X. M. Li and H. B. Zeng, *ACS Energy Lett.*, 2019, **4**, 673–681.
7 X. L. Xu, S. Y. Wang, Y. Chen, W. W. Liu, X. P. Wang, H. T. Jiang, S. Y. Ma and P. D. Yun, *ACS Appl. Mater. Interfaces*, 2022, **14**, 39524–39534.
8 C. Liu, H. Chen, P. Lin, H. H. Hu, Q. Y. Meng, L. B. Xu, P. Wang, X. P. Wu and C. Cui, *J. Mater. Sci.: Mater. Electron.*, 2022, **33**, 24895–24905.
9 Y. Y. Zhou and Y. X. Zhao, *Energy Environ. Sci.*, 2019, **12**, 1495–1511.
10 J. S. Manser, M. I. Saidaminov, J. A. Christians, O. M. Bakr and P. V. Kamat, *Acc. Chem. Res.*, 2016, **49**, 330–338.
11 H. W. Zhou, L. Fan, G. H. He, C. Yuan, Y. Y. Wang, S. Z. Shi, N. Sui, B. L. Chen, Y. T. Zhang, Q. X. Yao, J. S. Zhao, X. X. Zhang and J. Yin, *RSC Adv.*, 2018, **8**, 29089–29095.
12 M. Shen, Y. L. Zhang, B. L. Cheng, W. J. Ma, X. L. Huang, L. Zhang, Z. F. Chai and W. W. Lin, *CrystEngComm*, 2024, **26**, 3162–3166.
13 X. L. Huang, B. L. Cheng, W. J. Ma, S. M. Qi, Y. L. Zhang, M. Shen, T. Bo, L. Zhang and W. W. Lin, *Inorg. Chem.*, 2024, **63**, 11924–11929.
14 Q. Yao, J. M. Li, X. S. Li, Y. S. Ma, H. H. Song, Z. Y. Li, Z. G. Wang and X. T. Tao, *Adv. Mater.*, 2023, **35**, 2304938.
15 L. X. Yin, H. D. Wu, W. C. Pan, B. Yang, P. H. Li, J. J. Luo, G. D. Niu and J. Tang, *Adv. Opt. Mater.*, 2019, **7**, 1900491.
16 M. M. Yang, A. F. Li, X. Hao, L. L. Wu, W. B. Tian, D. Y. Yang and J. Q. Zhang, *Adv. Opt. Mater.*, 2023, **11**, 2203066.
17 M. A. Hadi, M. N. Islam and J. Podder, *RSC Adv.*, 2022, **12**, 15461–15469.
18 M. N. Islam, M. A. Hadi and J. Podder, *AIP Adv.*, 2019, **9**, 125321.
19 Q. Q. Jia, Z. X. Zhang, H. F. Ni, Q. Lin, G. Teri, P. G. Liu, J. Q. Luo, P. Z. Huang, Z. J. Wang, C. F. Wang, Z. Q. Liu, Y. Zhang and D. W. Fu, *Angew. Chem., Int. Ed.*, 2025, **64**, e202505163.
20 Q. Q. Jia, G. Teri, Q. F. Zhou, J. Q. Luo, H. F. Ni, P. Z. Huang, P. G. Liu, L. Pan, C. F. Wang, Z. Q. Liu, Z. X. Zhang, Y. Zhang and D. W. Fu, *Angew. Chem., Int. Ed.*, 2025, **64**, e202514669.
21 D. F. Wu, J. E. Zhou, W. Kang, K. An, J. Y. Yang, M. Zhou, P. He, Q. Huang and X. S. Tang, *J. Phys. Chem. Lett.*, 2021, **12**, 5110–5114.
22 D. W. Yang, F. Wang, S. Li, Z. F. Shi and S. F. Li, *J. Phys. Chem. C*, 2024, **128**, 2223–2230.
23 M. M. Yao, Q. Zhang, D. Wang, R. L. Chen, Y. C. Yin, J. Xia, H. Tang, W. P. Xu and S. H. Yu, *Adv. Funct. Mater.*, 2022, **32**, 2202894.
24 I. D. Brown, *Phys. Chem. Miner.*, 1987, **15**, 30–34.
25 B. L. Cheng, W. J. Ma, A. Tudi, F. F. Zhang, Z. L. Chen, X. L. Hou, Z. H. Yang and S. L. Pan, *Chem. Mater.*, 2023, **35**, 5671–5679.
26 B. L. Cheng, Z. J. Li, Y. Chu, A. Tudi, M. Mutailipu, F. F. Zhang, Z. H. Yang and S. L. Pan, *Natl. Sci. Rev.*, 2022, **9**, nwac110.
27 B. L. Cheng, W. J. Ma, A. Tudi, F. F. Zhang, X. F. Long, S. L. Pan and Y. Yang, *Mater. Today Chem.*, 2025, **45**, 102623.
28 J. Tauc, R. Grigorovici and A. Vancu, *Phys. Status Solidi*, 1966, **15**, 627–637.
29 (*a*) CCDC 2519961: Experimental Crystal Structure Determination, 2026, DOI: 10.25505/fiz.icsd.cc2ql72n; (*b*) CCDC 2519962: Experimental Crystal Structure Determination, 2026, DOI: 10.25505/fiz.icsd.cc2ql73p.